Original Article

JABFM Journal of Applied Biomaterials & Functional Materials

Lime-cement textile reinforced mortar (TRM) with modified interphase

Journal of Applied Biomaterials & Functional Materials
January-March: 1–9

DOI: 10.1177/2280800019827823
journals.sagepub.com/home/jbf
SAGE

Cesare Signorini[1,3], Antonella Sola[2], Andrea Nobili[2] and Cristina Siligardi[2]

Abstract

Background: Lack of interphase compatibility between the fabric and the matrix significantly impairs the load-bearing capacity of textile reinforced mortar (TRM). In this study, we consider the application of two inorganic surface coatings for enhancing the interphase bond properties.

Methods: Either of two silica-based coatings, namely nano- and micro-silica, were applied to alkali-resistant glass (ARG) and to hybrid carbon–ARG woven fabric. Mechanical performance of TRM reinforced with the uncoated and the coated fabric was compared in uniaxial tensile tests.

Results: Mechanical testing provides evidence of a remarkable enhancement in terms of ultimate strength and deformability for the coated specimens. This effect can be ascribed to the improved hydrophilicity of the fibers' surface and to the activation of pozzolanic reaction at the interphase. In addition, penetration of nano- and microparticles in the bundle of the textile yarns reduces the occurrence of telescopic failure.

Keywords

Inorganic coatings, textile reinforced mortar, interphase bond, silica

Date received: 17 November 2018; revised: 24 December 2018; accepted: 9 January 2019.

Introduction

Externally-bonded thin composite laminates, especially in the form of epoxy-based fabric reinforced polymers (FRP), are routinely employed to strengthen existing buildings.[1–4] For FRP composites, the development of reliable and consistent mechanical performance heavily hinges on the strong adhesion between the polymeric phase (i.e., epoxy resin) and the textile reinforcement (carbon, glass, aramid or basalt fabric).[5–7] Over the last two decades, a novel category of textile reinforced inorganic-matrix composite materials has attracted considerable attention, in light of the advantages it offers over FRP. These materials, known as textile reinforced concrete/mortar (TRC/TRM) or fabric reinforced cementitious matrix (FRCM), are obtained embedding the reinforcing fabric in cement and/or lime mortar.

Owing to the inorganic nature of the matrix, TRMs offer several advantages over FRPs. Indeed, they exhibit high compatibility with both concrete and masonry substrates, lower sensitivity to high temperatures and fire attacks, stability in humid environment (e.g. pipes, hydraulic infrastructure, off-shore structures etc.) and in the presence of pigmented surfaces. The latter feature is related to the intrinsic porosity of the mortar, which imparts high permeability to water vapor. Indeed, TRCs/TRMs are often preferred in delicate refurbishment interventions on historic masonry structures.[8] Intensive experimental activities have been carried out to assess the mechanical behavior of these laminates as strengthening elements for reinforced concrete (RC) beams, columns, arcs, slabs, and masonry panels.[9–12]

[1]Dipartimento di Scienze e Metodi dell'Ingegneria, Reggio Emilia, Italy
[2]Dipartimento di Ingegneria Enzo Ferrari, Modena, Italy
[3]Dipartimento di Economia Scienze e Diritto, Dogana, Republic of San Marino

Corresponding author:
Cesare Signorini, Dipartimento di Scienze e Metodi dell'Ingegneria, via G. Amendola, 2 - 42122 Reggio Emilia (RE), Italy.
Email: cesare.signorini@unimore.it

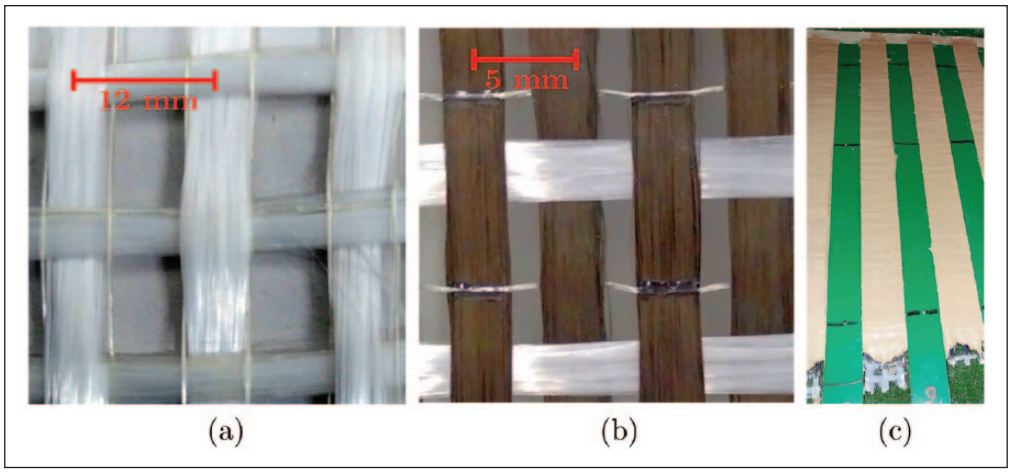

Figure 1. ARG fabric (a) and carbon fabric with ARG weft (b); G-MS laminates batch prior to moist curing (c).

On the other hand, the generally poor adhesion between the fabric and the mortar, especially when compared to FRP or steel reinforced concrete (S-FRCM), significantly impairs the wider adoption of TRMs in the engineering practice.[13,14] Indeed, delamination and telescopic failure occur much earlier, at low-load levels, and the remarkable mechanical performance of the fabric is put to little advantage. Furthermore, failure is generally inconsistent and characterized by large data scattering. The possibility of strengthening interphase adhesion has been the subject of many studies, in an attempt to bring TRM and TRC performance up to the level required for structural purposes. Several studies attempt to enhance the hydrophilicity (or wettability) of the fibers' surface and consequently establish a stronger chemical bond with the cement/lime mortar. Xu and Chung propose a technique for laying oxygen groups on the surface of carbon fibers,[15] while Li and colleagues provide evidence of interphase bond enhancement of polyethylene fibers immersed in a cementitious matrix by surface modification through plasma treatment.[16,17] Recently, promising results have appeared dealing with inorganic coating of multifilament fibers.[18,19] Yet, best performance is still obtained when epoxy coatings are considered. Butler et al. applied a polymeric sizing during the fibers' spinning process to eliminate surface defects and enhance durability in aggressive environments.[20] Messori et al. showed that epoxy micro-coatings prevent telescopic failure altogether and that the overall mechanical performance is strongly affected by the coating thickness and formulation.[21] The effect of high temperature exposure was also investigated.[22]

In this work, we present an experimental investigation on the mechanical behavior of TRM laminates in uniaxial tensile tests. The performance is assessed of two silica-based coatings, namely micro- and nanosilica, applied to two reinforcing fabrics, namely alkali-resistant glass (ARG) and high-tenacity carbon with ARG weft (C), embedded in a single cement-lime hybrid mortar. Preliminary design considerations are put forward through statistical analysis of the experimental evidence. The final goal is to promote wider acceptance of interphase-modified TRM composite materials in current engineering practice.

Materials and methods

Materials

Thin one-ply sandwich laminates were manually manufactured by wet laying-up multifilament woven fabrics in a commercially available hybrid structural lime-cement mortar. Two different thermo-welded textiles are used as reinforcing phases: a balanced open-square-mesh biaxial ARG fabric (Figure 1(a)) and a uniaxial high-tenacity carbon fabric with ARG yarns in the weft (Figure 1(b)). The main mechanical properties of the fabrics are reported in Table 1. A cement–lime hybrid mortar is used as embedding agent, characterized by fine aggregates ($\leq$1.4 mm), whose properties are described in Messori et al.[21]

Surface modifications

Two different silica-based coatings are applied directly to the ARG and carbon fabric by immersion and silica deposition.

Nanosilica deposition. Nanosilica (NS) deposition was achieved using a sol–gel technique. To coat 450 cm^2 of ARG fabric (as required for five specimens), 30 mL of tetraethyl orthosilicate (TEOS 98%, Sigma Aldrich) precursor are stirred with 48 mL of 2-propanol at 50°C for 15 min in a lidded beaker. Successively, 12 mL of deionized water and 1.5 mL of nitric acid are added to the solution and stirred for 2 h. Cut-to-size fabric is dipped in the

Table 1. Multifilament AR-glass (G) and carbon (C) fabric properties.

Feature	Unit	G	C
Yarn count	tex (g/km)	1200	800
Warp	—	AR-glass	HT-carbon
Specific weight (warp, per unit area)	g/m^2	150	150
Weft	—	AR-glass	AR-glass
Specific weight (weft, per unit area)	g/m^2	150	50
Density of the fibers (warp)	g/cm^3	2.50	1.78
Nominal warp grid spacing	mm	12	5
Equivalent thickness, t_f	μm	60	89
Ultimate strength with epoxy (warp)	MPa	1200	3500
Elastic modulus	GPa	74	240

Table 2. Coupon geometry for tensile testing.

Feature	Unit	G	C
Coupon length, L	mm	450	450
Gauge length, L_g	mm	250	250
Edge tabs length	mm	100	100
Width, w_g	mm	36	35
Yarns per coupon	—	3	7
Fiber effective area,[27] A_f	mm^2	2.16	3.10
Total thickness	mm	7	7

solution for 5 min and then carefully rinsed with distilled water upon extraction. Finally, the wet fabric is left to dry in an oven at 105°C for 15 min.[23]

Microsilica deposition. Silica microparticles (particle size: 0.15 μm) are laid onto the fabric surface starting from a silica-fume dispersion (hereafter "microsilica,", labelled "MS"). The suspension is obtained from a commercially available silica fume dry powder (Elkem Silicon Materials, Bluestar Company) with a minimum purity grade of 85%. In order to coat 450 cm^2 of glass fabric, 80 g of undensified silica-fume powder are gradually added to 80 mL of deionized water and stirred for 1 h in a lidded beaker at ambient temperature. The obtained suspension is sonicated for 10 min (Elmasonic S30H) immediately prior to fabric coating, partly following the guidelines provided by Hommer,[24] although in a different context. Cut-to-size fabric is dipped in the suspension for 5 min. Finally, fabrics are left to dry at ambient conditions for 24 h, until complete evaporation of water occurs.

Specimen preparation

Rectangular laminates for tensile tests (coupons) are manufactured according to the protocol documented in the previous works,[23,25] which complies with the ICC AC434 guidelines.[26] A polyethylene modular mold is used to cast each coupon individually. A silicon-based lubricant is sprayed on the bottom surface of the form-work before applying the first layer of fresh mortar, in order to ease extraction (stripping). To achieve uniform thickness and evenness of the mortar layers, polyethylene constraining laths are pinned at equispaced distance, either 36 mm for glass or 35 mm for carbon coupons. Indeed, the width of specimens is designed to accommodate three ARG warp yarns and seven carbon warp yarns, respectively. Then, the fabric is laid and slightly pressed onto the fresh mortar. A second level of laths is pinned on top of the first and a second layer of mortar is applied accordingly. Specimens, wrapped in polypropylene foil, undergo moist curing for 7 days. Successively, they are extracted from the formwork and left to cure in ambient conditions for 50 days. A few days before testing, two pairs of 100-mm-long CFRP tabs are glued at the specimen ends to accommodate the universal testing machine (UTM) grips. Geometrical and mechanical characteristics of the specimens are summarized in Table 2. The effective cross-sectional area of the laminate, A_f, through which strength is related to stress, is computed according to equation (2.6) of CNR-DT200/2004.[27]

Testing procedure

The mechanical behavior was assessed through uniaxial tensile tests in an electromechanical UTM equipped with a 30 kN load cell and two wedge clamps. Tests were carried out under displacement control at a nominal elongation rate of 2 mstrain/min. The actual elongation rate was determined through digital image correlation in a 3 megapixel stereoscopic Dantec Dynamics optical system (Q-400). Previous analysis shows that the actual displacement rate is decreased by grip elongation of about 10% with respect to the nominal ramp and this contribution cannot be disregarded for accurate evaluation of the strain and of the moduli.[23,25,28,29] Failed specimens were investigated in an optical stereo-microscope (Leica EZ4D) and in a scanning electron microscope (SEM) (Quanta-200, Fei Company, Oxford Instruments) to qualitatively assess interphase enhancement. A minimum of four specimens is considered in each test group.

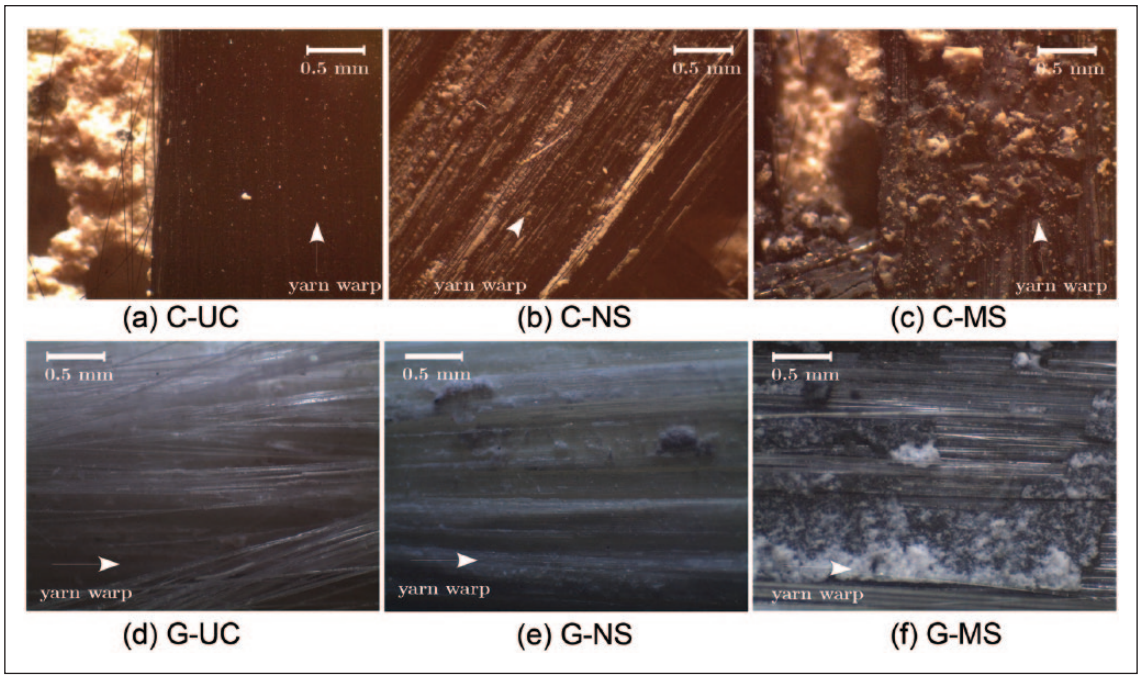

Figure 2. Images (35× magnification) of the uncoated (UC), nanosilica (NS), and microsilica (MS) coated carbon (a–c) and glass fabric (d–f) after failure.

Design considerations

Statistical analysis of the mechanical performance is carried out in order to evaluate characteristic values for ultimate strength and strain of uncoated and coated specimens. In particular, data scattering plays a crucial role when moving to design values. According to ICC AC434,[26] when failure occurs in tension, the design tensile strain is given by

$$\varepsilon_{f,d} = 0.70\,\varepsilon_{fu,k} \le 12 \text{ mstrain}, \quad (1)$$

where $\varepsilon_{fu,k}$ is the characteristic tensile strain of the TRM laminate

$$\varepsilon_{fu,k} = \mu(\varepsilon_{fu}) - 1.96\,\sigma(\varepsilon_{fu}). \quad (2)$$

In equation (2), $\mu(\cdot)$ and $\sigma(\cdot)$ denote the mean and the standard deviation of the relevant quantity, respectively. This formula really yields a characteristic value for strain (i.e., the 5% fractile of the sample set) inasmuch as the latter follows a normal distribution. The design ultimate strength at failure is evaluated according to

$$f_{f,d} = 0.70 f_{fu,k}, \quad (3)$$

where $f_{fu,k}$ is the characteristic ultimate strength, which may be computed from the characteristic ultimate strain via E_f, the cracked modulus of the TRM,[25]

$$f_{fu,k} = 0.85 E_f \varepsilon_{fu,k}. \quad (4)$$

Results and discussion

Optical and SEM investigation

Representative 35× magnification pictures of the failed C-UC, C-NS (taken from a previous work),[23] and C-MS specimens are reported in Figure 2(a) to (c). Uncoated specimens present little evidence of mortar adhesion to the fibers' surface, which appears completely clean. Conversely, both silica coatings seem to induce a strong coupling effect at the interphase, since mortar patches remain diffusely attached to the coated fabric after failure. Analogous considerations hold true for glass-fabric reinforced specimens, as shown in Figure 2(d) to (f). To gain further insight into the adhesion enhancement provided by the coatings, scanning electron microscopy (SEM) images are presented in Figure 3. The strong bond at the interphase may be ascribed to pozzolanic reactions occurring between the cementitious matrix and the finely dispersed silica particles.[30] Pozzolanic activity is promoted by silica-rich precursors reacting with calcium hydroxide ($Ca(OH)_2$) and silicic acid ($Si(OH)_4$) to obtain calcium silicate hydrate ($CaH_2SiO_4.2H_2O$), which presents good binding properties. The strongly alkaline environment of the cementitious matrix promotes pozzolanic reaction and its stability.[31] In fact, silica fume is largely employed as additive in high performance concrete because of its strong pozzolanic reactivity. Furthermore, silica fume enhances the compressive strength of concrete and mortar as well as the durability and rheology of the conglomerate.[32]

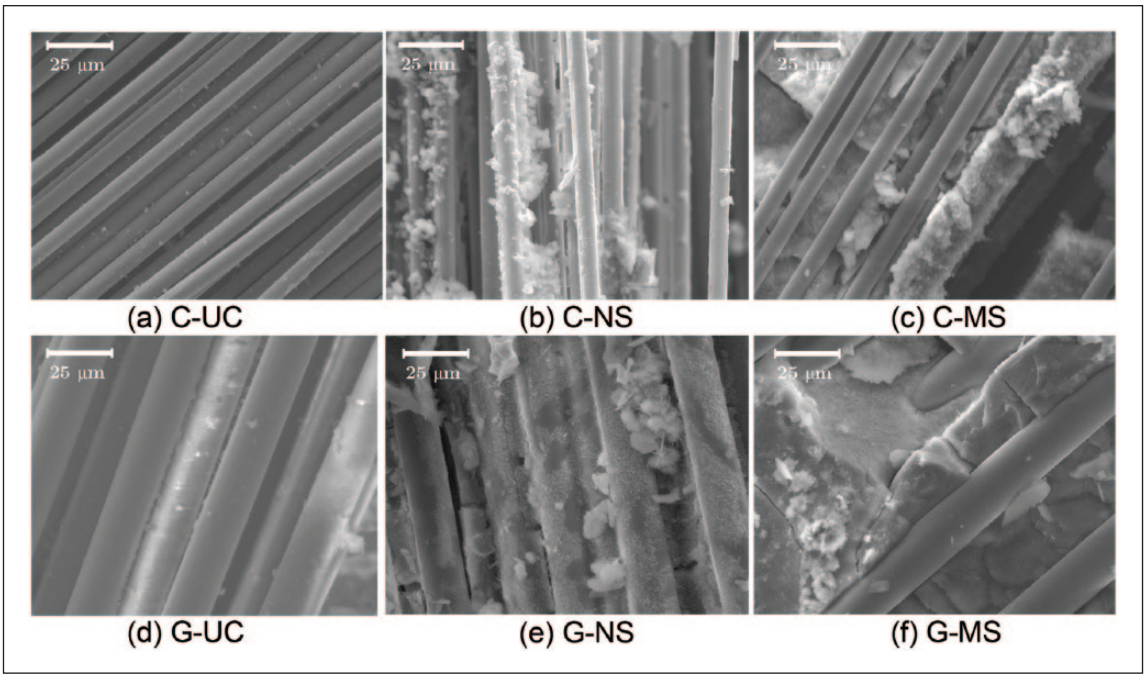

Figure 3. SEM images of uncoated (UC), nanosilica (NS), and microsilica (MS) coated carbon (a–c) and glass (d–f) specimens after failure.

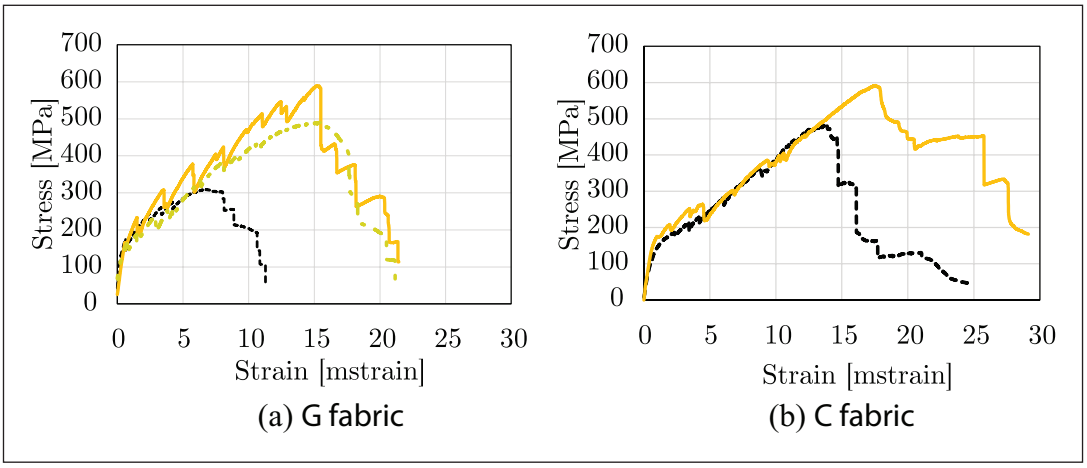

Figure 4. The mean stress–strain curves for glass (a) and carbon (b) samples: uncoated group (black, dotted), NS coated group (green, dash-dotted, only for ARG samples) and MS coated group (orange, solid).

Mechanical tests

Figure 4 gathers the mean stress–strain curves evaluated for each specimen group and it appears that the improvement in terms of ultimate strain, due to coating, is remarkable for both fabrics. An equally impressive increase is seen for the ultimate stress for glass, while the beneficial effect for carbon is milder. Looking at the slope of the plots, we note little change in the uncracked (and, possibly, in the cracked) modulus of the coated groups, as compared to the relevant uncoated group. Indeed, in the first part of the stress–strain curve, the elastic (uncracked) modulus is mainly driven by the uncracked mortar, which provides the main contribution to the overall stiffness. As expected, coating has little bearing on the stiffness of the uncracked mortar. Successively, once the matrix is fully cracked, the coupon stiffness is governed by that of the dry fabric and the contribution of the deposited nano- and microparticles is negligible. Nonetheless, the improved interphase is responsible for the higher ultimate tensile strength and elongation of the laminate at failure. In fact, the coupling effect induced by the coating increases the resistance against the sliding mechanisms at the interphase and it promotes the formation of a diffuse crack pattern throughout

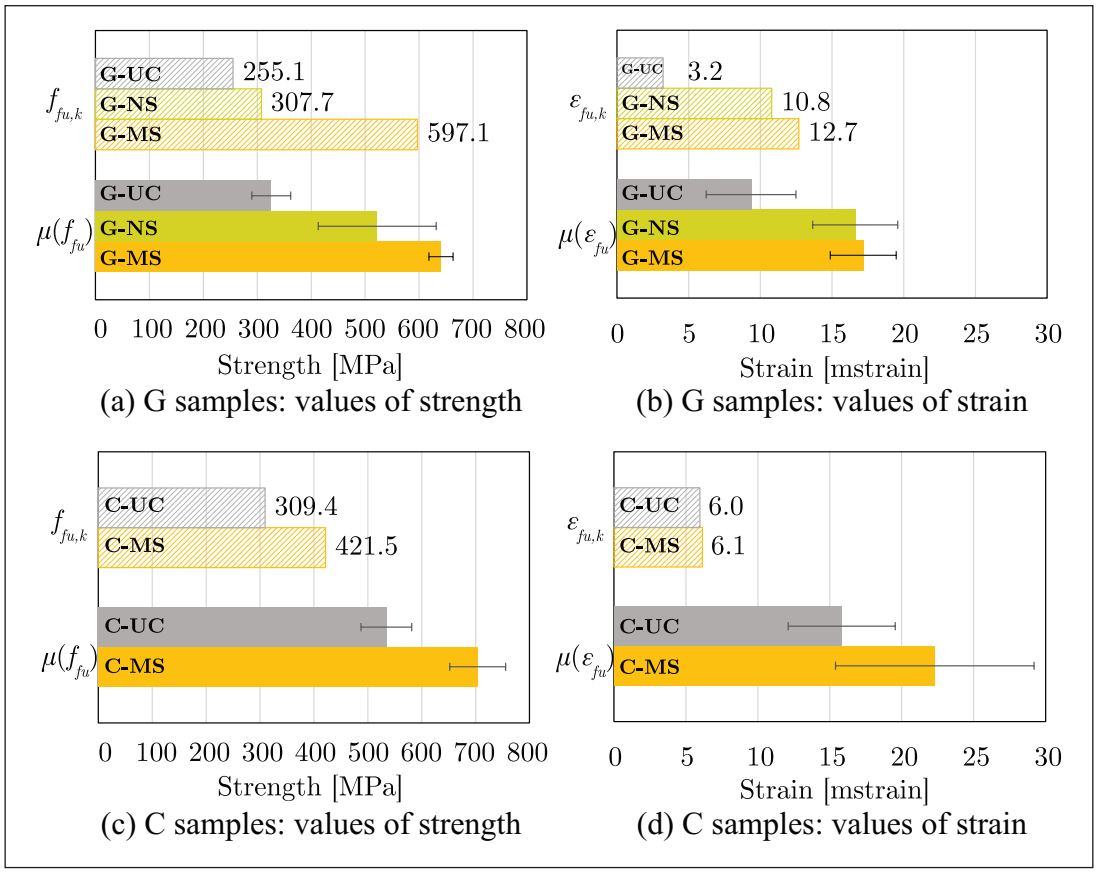

Figure 5. Mean ultimate values with ±1 standard deviation bands and characteristic values for uncoated (UC, grey), nanosilica-coated (NS, green) and microsilica-coated (MS, orange) specimens for each test group.

the length of the laminate. This contribution manifests itself after matrix cracking and gradually disappears at the fully cracked stage. The mean curves are representative of the performance enhancement for both G and C reinforcements. For carbon fibers, these outcomes are consistent with the study carried out by Nadiv et al.[19] They performed double-sided pull-out tests on uncoated, micro- and nano-silica-coated single carbon yarns embedded in a Portland cement mortar. According to Nadiv et al.,[19] the presence of pozzolan particles penetrating the bundle of fabric yarns induces a relevant increase in mechanical performance in terms of pull-out force. As anticipated, microsilica coating brings higher beneficial effects when applied to glass rather than carbon fabric. This outcome may be ascribed to the superior compatibility between microsilica and silica-based fibers, as opposed to carbon fibers. Considering nanosilica, a trend similar to that found in a previous study is observed by which the effectiveness of the nano-coating seems likewise governed by the chemical nature of the fibers.[23] Indeed, when ARG fabric is considered, a double-sided coupling effect is established (i.e., fibers–silica and silica–matrix), thanks to the pozzolanic reactions that are likely to occur. This coupling promotes a stable interphase layer of silicates that strengthens the composite material.

The bar-charts of Figure 5 provide characteristic and mean values for the ultimate stress and elongation for G and C fabrics. Data scattering is given through ±1 standard deviation bars. The mean, design (cf. equation (1)) and characteristic (cf. equation (2)) values for G and C samples are reported in Table 3. This table presents the ultimate strength and strain values and their relative increment, referred to as $\Delta(\cdot)$, with respect to the uncoated specimen, alongside the coefficient of variation $\mathrm{CV}(\cdot)$. Looking at the ARG fabric, we observe that the gain in terms of ultimate elongation in the silica group with respect to the uncoated group is almost equal to the benefit achieved with microsilica. This behavior is due to microcrack formation on the surface of the coupon, which allows to dissipate a vast amount of mechanical energy.[29] Despite the undeniable increase of mechanical performance achieved in the coated groups, the ultimate strength of the dry fabric could not be reached and failure of the composite system still occurs through sliding at the interphase. This classical collapse mechanism (well described by the recent CNR Technical Document 215/18[33]) takes place in combination with telescopic failure, namely the differential displacement between the inner (core) and the outer (sleeve) filaments in the yarns. In fact, the internal filaments are poorly

Table 3. Ultimate tensile strength and design limits for all tested groups.

Group	$\mu(f_{fu})$	$\sigma(f_{fu})$	$CV(f_{fu})$	$\Delta(f_{fu})$	$f_{fu,k}$ (equation (4))	$f_{f,d}$ (equation (3))	$\Delta(f_{fu,k})$
	(MPa)	(MPa)	(%)	(%)	(MPa)	(MPa)	(%)
G-UC	325.8	36.1	11.1	—	255.1	178.5	—
G-NS	522.3	109.4	21.0	+60.3	307.7	215.4	+20.7
G-MS	640.8	22.3	3.5	+96.7	597.1	418.0	+134.1
C-UC	534.3	47.1	8.8	—	442.0	309.4	—
C-MS	703.8	51.9	7.4	+31.7	602.1	421.5	+36.2
Group	$\mu(\varepsilon_{fu})$	$\sigma(\varepsilon_{fu})$	$CV(\varepsilon_{fu})$	$\Delta(\varepsilon_{fu})$	$\varepsilon_{fu,k}$ (equation (2))	$\varepsilon_{f,d}$ (equation (1))	$\Delta(\varepsilon_{fu,k})$
	[μstrain]	[μstrain]	(%)	(%)	[μstrain]	[μstrain]	(%)
G-UC	9.3	3.1	33.4	—	3.2	2.3	—
G-NS	16.6	3.0	17.9	+77.7	10.8	7.6	+235.1
G-MS	17.2	2.3	13.4	+83.8	12.7	8.9	+293.5
C-UC	15.8	3.7	23.5	—	8.5	6.0	—
C-MS	22.3	6.9	30.9	+40.9	8.8	6.1	+2.9

bonded to the surrounding matrix and are therefore prone to slide over the external filaments.

Conclusions

An experimental investigation concerning the mechanical performance of coated AR-glass and carbon TRM systems is presented. Two sustainable inorganic silica-based coatings, namely micro- and nanosilica (MS and NS, respectively), are considered for the reinforcing fabric, which is embedded in a hybrid lime-cement matrix. Coating fosters a concentrated pozzolanic reaction at the fabric-to-matrix interphase and thereby promotes chemical bond formation.[19,34] The role of the coating is assessed qualitatively through optical and electron microscopy and quantitatively in uniaxial tensile tests, according to the ICC AC434 guidelines. Design considerations are given in terms of ultimate strength and elongation. Both MS and NS coatings appear to effectively address the poor bond formation issue that affects inorganic matrix composites. Indeed, they impart remarkable strength improvement over the uncoated specimens, especially when applied to glass fabric. Besides, in contrast to epoxy coatings, this technology retains the important advantages connected with an inorganic agent, namely high-temperature resistance,[35,36] compatibility and durability, and water vapor permeability.[37] With respect to other available technologies, such as impregnation with partially organic primers at the lamination stage,[25] it affords standardization and industrialization and consequently a reliable and consistent performance. In summary, the following conclusions can be drawn:

- Nano- and microsilica particles induce a substantial increase in terms of ultimate strength and elongation for TRM.
- The remarkable improvement in mechanical performance can be ascribed to pozzolanic activity, concentrated at the interphase between the fabric and the matrix.
- Coating produces little effect on the uncracked modulus, which is dominated by the inorganic matrix stiffness, as well as on the cracked modulus, which is related to the dry fabric stiffness.
- Both coatings convey the advantages connected to an inorganic material alongside the ease of application of a "pre-preg" technology. Indeed, dry coating is prone to industrialization as opposed to on-site treatments with primers or resins.
- Silica coating appears more performing in connection to glass fabric, as a consequence of the superior chemical affinity with glass and of the related two-way connection at the interphase. This strong bridging impacts on data scattering, which is highest for C-MS as compared to G-NS and G-MS specimens.
- Compared to uncoated specimens, surface modification produces a remarkable reduction of data scattering, which, in turn, markedly improves the design limits. Indeed, a more than two-fold increase in terms of design elongation is achieved for the coated specimens and this outcome is mainly ascribed to the sharp reduction in terms of standard deviation. In fact, the coefficient of variation decreases from 33% for G-UC to 18% for G-NS and to 13% for G-MS.

Acknowledgements

This work is an outgrowth of the poster awarded at the Zwick Academia Day, Rome 2018: We gratefully thank Dr. Robert Strehle, Dr. Tania Pesalovo, Dr. Paolo Sacchetti and the Zwick Roell Group for organizing such pleasant event. Authors

acknowledge the contribution of Prof. Roberto Giovanardi and Dr. Andrea Cattini in performing the optical microscopy investigation.

Declaration of Conflicting Interest

The authors declared no potential conflicts of interest with respect to the research, authorship, and/or publication of this article.

Funding

The authors disclosed receipt of the following financial support for the research, authorship, and/or publication of this article: This work was supported by "FAR dipartimentali 2016" [Decr. 73/2017, prot. 37510], which AN gratefully acknowledges.

ORCID iD

Cesare Signorini https://orcid.org/0000-0002-6867-1340

References

1. Nanni A. Concrete repair with externally bonded FRP reinforcement. *Concr Int* 1995; 17: 22–26.
2. Khalifa A, Gold WJ, Nanni A, et al. Contribution of externally bonded FRP to shear capacity of RC flexural members. *J Compos Constr* 1998; 2: 195–202.
3. Triantafillou TC and Papanicolaou CG. Shear strengthening of reinforced concrete members with textile reinforced mortar (TRM) jackets. *Mater Struct* 2006; 39: 93–103.
4. Triantafillou TC. Strengthening of masonry structures using epoxy-bonded FRP laminates. *J Compos Constr* 1998; 2: 96–104.
5. Tsai SW and Hahn TH. *Introduction to composite materials*. Basel, Switzerland: Technomic Publishing AG, 1980.
6. Gay D and Hoa SV. *Composite materials: design and applications*. Boca Raton, FL: CRC Press, 2007.
7. Tirillò J, Ferrante L, Sarasini F, et al. High velocity impact behaviour of hybrid basalt-carbon/epoxy composites. *Compos Struct* 2017; 168: 305–312.
8. Nobili A and Falope F. Impregnated carbon fabric-reinforced cementitious matrix composite for rehabilitation of the Finale Emilia hospital roofs: case study. *J Compos Constr* 2017; 21: 05017001.
9. Ascione L, de Felice G and De Santis S. A qualification method for externally bonded fibre reinforced cementitious matrix (FRCM) strengthening systems. *Composites Part B* 2015; 78: 497–506.
10. Donnini J, Lancioni G and Corinaldesi V Failure modes in FRCM systems with dry and pre-impregnated carbon yarns: experiments and modeling *Composites Part B* 2018; 140: 57–67.
11. Alecci V, Focacci F, Rovero L, et al. Extrados strengthening of brick masonry arches with PBO-FRCM composites: experimental and analytical investigations. *Compos Struct* 2016; 149: 184–196.
12. Trapko T, Urbańska D and Kamiński M. Shear strengthening of reinforced concrete beams with PBO-FRCM composites. *Composites Part B* 2015; 80: 63–72.
13. Falope F, Lanzoni L and Tarantino A. Modified hinged beam test on steel fabric reinforced cementitious matrix (SFRCM). *Composites Part B* 2018; 146: 232–243.
14. Falope F, Lanzoni L and Tarantino A. Double lap shear test on steel fabric reinforced cementitious matrix (SFRCM). *Compos Struct* 2018; 201: 503–513.
15. Xu Y and Chung D. Carbon fiber reinforced cement improved by using silane-treated carbon fibers. *Cem Concr Res* 1999; 29: 773–776.
16. Li VC, Wu HC and Chan YW. Effect of plasma treatment of polyethylene fibers on interface and cementitious composite properties. *J Am Ceram Soc* 1996; 79: 700–704.
17. Li V and Stang H. Interface property characterization and strengthening mechanisms in fiber reinforced cement based composites. *Adv Cem Based Mater* 1997; 6: 1–20.
18. Scheffler C, Gao S, Plonka R, et al. Interphase modification of alkali-resistant glass fibres and carbon fibres for textile reinforced concrete i: Fibre properties and durability. *Compos Sci Technol* 2009; 69: 531–538.
19. Nadiv R, Peled A, Mechtcherine V, et al. Micro-and nanoparticle mineral coating for enhanced properties of carbon multifilament yarn cement-based composites. *Composites Part B* 2017; 111: 179–189.
20. Butler M, Mechtcherine V and Hempel S. Durability of textile reinforced concrete made with AR glass fibre: effect of the matrix composition. *Mater Struct* 2010; 43: 1351–1368.
21. Messori M, Nobili A, Signorini C, et al. Mechanical performance of epoxy coated AR-glass fabric textile reinforced mortar: influence of coating thickness and formulation. *Composites Part B* 2018; 149: 135–143.
22. Messori M, Nobili A, Signorini C, et al. Epoxy-coating degradation in glass textile reinforced mortar (GTRM) composites after high temperature exposure. *Constr Build Mater* 2019; under review.
23. Signorini C, Nobili A, Cedillo Gonzalez EI, et al. Silica coating for interphase bond enhancement of carbon and AR-glass textile reinforced mortar (TRM). *Composites Part B* 2018; 141: 191–202.
24. Hommer H. Interaction of polycarboxylate ether with silica fume. *J Eur Ceram Soc* 2009; 29: 1847–1853.
25. Nobili A and Signorini C. On the effect of curing time and environmental exposure on impregnated carbon fabric reinforced cementitious matrix (cfrcm) composite with design considerations. *Composites Part B* 2017; 112: 300–313.
26. ICC Evaluation Service. *Acceptance criteria for masonry and concrete strengthening using fiber-reinforced cementitious matrix (FRCM) composite systems*. Report no. AC434, 2013. Whittier, CA: ICC Evaluation Service.
27. Italian National Research Council (CNR).*Guide for the design and construction of an externally bonded FRP system for strengthening existing structures*. Technical document no. 200. Rome: CNR, 2004.
28. Nobili A. Durability assessment of impregnated glass fabric reinforced cementitious matrix (GFRCM) composites in the alkaline and saline environments. *Constr Build Mater* 2016; 105: 465–471.

29. Signorini C, Nobili A and Falope FO. Mechanical performance and crack pattern analysis of aged carbon fabric cementitious matrix (CFRCM) composites. *Compos Struct* 2018; 202: 1114–1120.
30. Sanchez F and Sobolev K. Nanotechnology in concrete–a review. *Constr Build Mater* 2010; 24: 2060–2071.
31. Cherian C and Arnepalli D. A critical appraisal of the role of clay mineralogy in lime stabilization. *Int J Geosynth Ground Eng* 2015; 1: 8.
32. Qing Y, Zenan Z, Deyu K, et al. Influence of nano-SiO_2 addition on properties of hardened cement paste as compared with silica fume. *Constr Build Mater* 2007; 21: 539–545.
33. Italian National Research Council (CNR). *Istruzioni per la progettazione, l'esecuzione ed il controllo di interventi di consolidamento statico mediante l'utilizzo di compositi fibrorinforzati a matrice inorganica*. Technical document no. 215. Rome: CNR, 2018.
34. Jo BW, Kim CH, Tae G, et al. Characteristics of cement mortar with nano-SiO_2 particles. *Constr Build Mater* 2007; 21: 1351–1355.
35. Trapko T The effect of high temperature on the performance of CFRP and FRCM confined concrete elements. *Composites Part B* 2013; 54: 138–145.
36. Donnini J, De Caso y Basalo F, Corinaldesi V, et al. Fabric-reinforced cementitious matrix behavior at high-temperature: experimental and numerical results. *Composites Part B* 2017; 108: 108–121.
37. Garmendia L, San-José JT, Garca D, et al. Rehabilitation of masonry arches with compatible advanced composite material. *Constr Build Mater* 2011; 25: 4374–4385.